

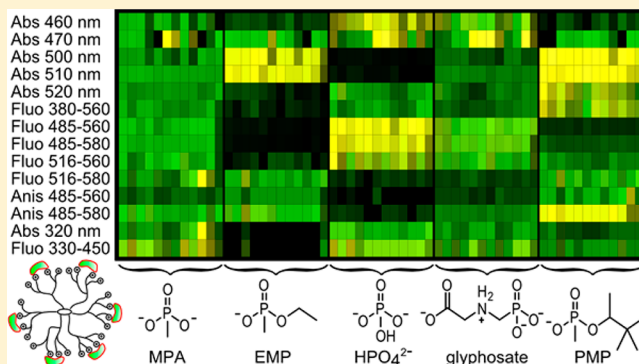
# A Supramolecular Sensing Array for Qualitative and Quantitative Analysis of Organophosphates in Water

Yuanli Liu and Marco Bonizzoni\*

Department of Chemistry, The University of Alabama, P.O. Box 870336, Tuscaloosa, Alabama 35487-0336, United States

**S** Supporting Information

**ABSTRACT:** The organophosphate class of compounds includes common herbicides as well as highly toxic nerve gases whose detection is important from an environmental and a public safety perspective. We describe here a fluorescence turn-on sensor array for the rapid detection and quantitation of relevant organophosphates in neutral water. The array elements self-assemble from commercially available dyes and PAMAM dendrimers, and sensing is based on an indicator displacement assay. Data interpretation through pattern recognition methods (PCA, LDA) showed excellent cluster separation and sample classification. In addition, we were also able to use this system for simultaneous differentiation and quantitative analysis of methylphosphonate (a nerve gas byproduct), glyphosate (a ubiquitous herbicide), and inorganic phosphate over a wide range of concentrations (10  $\mu$ M to 2 mM).



## INTRODUCTION

Organophosphates are a class of compounds frequently used as herbicides, pesticides and chemical warfare agents. Glyphosate is an example of an organophosphate widely used as herbicide in agriculture,<sup>1</sup> whose overuse causes adverse effects to animals<sup>2</sup> and aquatic vegetation,<sup>3</sup> and may cause the proliferation of breast cancer in humans.<sup>4</sup> Another important class of organophosphates are the sarin, soman, and VX nerve agents, extremely toxic chemical warfare agents that act as non-competitive acetylcholinesterase inhibitors.<sup>5</sup>

The widespread use of organophosphate herbicides and the public safety concern regarding chemical warfare agents have made the detection and quantitative determination of organophosphates and their degradation products a very desirable goal. Numerous attempts have been made to develop such methods.<sup>6</sup> Instrumental analyses such as chromatography and mass spectrometry are most frequently used;<sup>7</sup> these approaches, however, require large and expensive instruments and trained operators. Other methods have also been proposed, such as fluorescent<sup>8</sup> and colorimetric detection,<sup>9</sup> the use of carbon nanotubes,<sup>10</sup> electrochemical analysis,<sup>11</sup> surface acoustic wave devices,<sup>12</sup> microcantilevers,<sup>13</sup> and protein nanopores.<sup>14</sup> Although significant progress has been made, these techniques have not yet met the demands of throughput, cost, sensitivity and ease of operation.

Array sensing techniques<sup>15</sup> have been recently applied in this field as well, leading to examples of detection of herbicides,<sup>16</sup> nerve agent simulants and other toxic gases.<sup>17</sup> However, the systems reported so far crucially rely on complex, highly specialized molecular probes that impose a significant synthetic

burden on the prospective user; simpler methods with comparable or improved detection capability are highly desirable.

We have previously demonstrated that a sensing ensemble assembled from a hyperbranched polymer and a fluorescent dye is able to discriminate biologically relevant phosphates in neutral water using multivariate detection.<sup>18</sup> Inspired by that work, we have developed a fluorescent turn-on sensing array that can differentiate organophosphate herbicides and nerve agent related compounds in water solution at neutral pH. The compound panel on which we focused is shown in Figure 1. In addition to the herbicide glyphosate (Roundup), we included pinacolyl methyl phosphonate (PMP) and ethyl methylphosphonate (EMP)

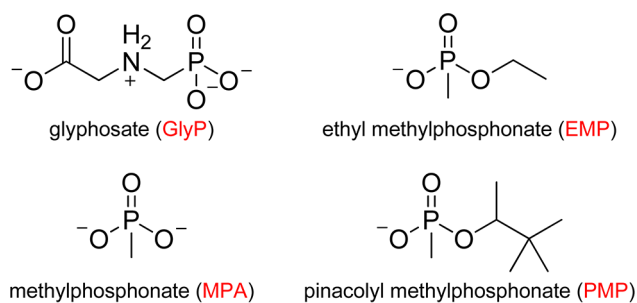


**Figure 1.** Organophosphates targeted in this study, shown in their protonation state in water at pH 7.4.

Received: August 1, 2014

Published: September 8, 2014

onate (EMP), the immediate degradation products of soman and agent VX, respectively. Methylphosphonate was also included because this compound is formed by hydrolysis of organophosphate nerve agents and of byproducts of nerve gas manufacture;<sup>19</sup> as such, its presence is excellent evidence of the use, storage or manufacture of these chemical warfare agents.<sup>20</sup>

To the best of our knowledge, this is the first array sensing system assembled from commercially available building blocks that can detect a wide range of organophosphates including compounds relevant as herbicides and as evidence of nerve gas manufacture and use. Moreover, the proposed sensing system functions in neutral water, typically a challenging medium for supramolecular sensing, but the most relevant to practical analysis of such target compounds.

## RESULTS AND DISCUSSION

Our supramolecular sensing system employs an indicator displacement assay<sup>21</sup> based on the displacement of a dye from a host–dye complex (Figure 3). An amine-terminated poly(amidoamine) (PAMAM) dendrimer with 1,2-diaminoethane core was used as the host. These polycationic polymers are known to uptake dye molecules<sup>22</sup> and phosphates.<sup>23</sup> We used a generation 5 (G5) PAMAM dendrimer as we found this size to be the best compromise between high binding affinity and affordability; in fact, smaller dendrimers display too low binding affinity for the target anions for use at micromolar concentration. On the other hand, although larger dendrimers may display higher affinity for the phosphate analytes, their high cost would be a significant drawback for the practicability of the proposed method.

We then chose fluorescein (F) and 4-methylumbelliferyl phosphate (MUP), both highly fluorescent dianions in water at neutral pH (Figure 2), to construct two dendrimer–dye

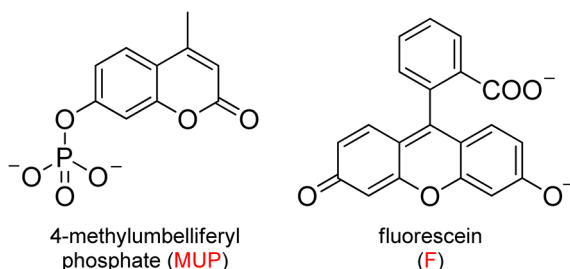


**Figure 2.** Fluorescent indicators used in the dendrimer–dye sensing elements of the proposed sensing array.

complexes, ( $G5 \bullet F_n$ ) and ( $G5 \bullet MUP_m$ ), to use as the sensing elements in a two-member sensor array. The fluorescence of fluorescein and 4-methylumbelliferyl phosphate is quenched upon binding to G5 (see Supporting Information). In the presence of the target organophosphates, the indicators are displaced from their complex and their fluorescence is revived (Figure 3). For a given analyte concentration, the extent of displacement and fluorescence recovery depend on the affinity of each guest for the dendrimer host.

All experiments presented hereafter have been carried out in water solution buffered to pH 7.4 with HEPES (50 mM). A fluorescence titration experiment was performed to confirm the displacement behavior; a representative example is shown in Figure 4. The emission of fluorescein is first quenched upon binding to G5 to form the sensing ensemble ( $G5 \bullet F_n$ ). The ( $G5 \bullet F_n$ ) complex then displays fluorescence turn-on behavior

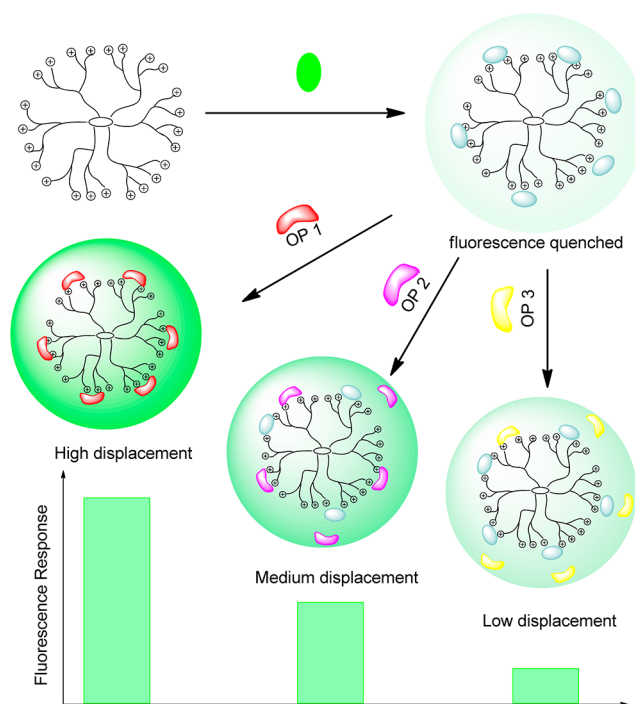


**Figure 3.** Schematic illustration of fluorescence modulation caused by the competitive binding between the quenched G5–dye complexes and the organophosphate analytes.

in the presence of methylphosphonate (MPA). Figure 4 (bottom) shows that the emission is dramatically revived by the addition of aliquots of MPA to a solution of the ( $G5 \bullet F_n$ ) sensing ensemble, until the emission of free fluorescein is reached, indicating that MPA has fully displaced the indicator from the dendrimer–indicator complex. Comparable results were obtained with 4-methylumbelliferyl phosphate (MUP, see Supporting Information).

Similar fluorescence titrations were also carried out for glyphosate (GlyP), ethyl methylphosphonate (EMP), pinacolyl methylphosphonate (PMP) and  $Na_2HPO_4$  to test the response of the ( $G5 \bullet F_n$ ) sensing ensemble to our panel of analytes. The five targets display differential displacement behavior, as indicated by the fluorescence recovery profiles shown in Figure 5, but the ( $G5 \bullet F_n$ ) sensing ensemble alone is not quite capable of differentiating these analytes. To capture more information, we turned to 4-methylumbelliferyl phosphate (MUP, see Figure 2). This dye is commonly used in biological applications,<sup>24</sup> and it is of particular interest to us because it contains a phosphate moiety that makes it similar to our target analytes. Sensing ensembles ( $G5 \bullet F_n$ ) and ( $G5 \bullet MUP_m$ ) were then employed to construct a sensor array, which was used for qualitative as well as quantitative recognition studies of organophosphates.

We monitored the response of the ( $G5 \bullet F_n$ ) and ( $G5 \bullet MUP_m$ ) ensembles in the presence of organophosphates through absorbance, fluorescence intensity and fluorescence anisotropy measurements at different wavelengths. These studies were conducted on a multimode microwell plate reader for rapid data acquisition in an array format. We first tested the two-component sensor array with the five selected phosphates at 800  $\mu M$  analyte concentration. Twelve replicates of each sample were measured. The raw experimental response is summarized visually in Figure 6 (see also Supporting Information for further details). The rich differential information contained in the response was evaluated using

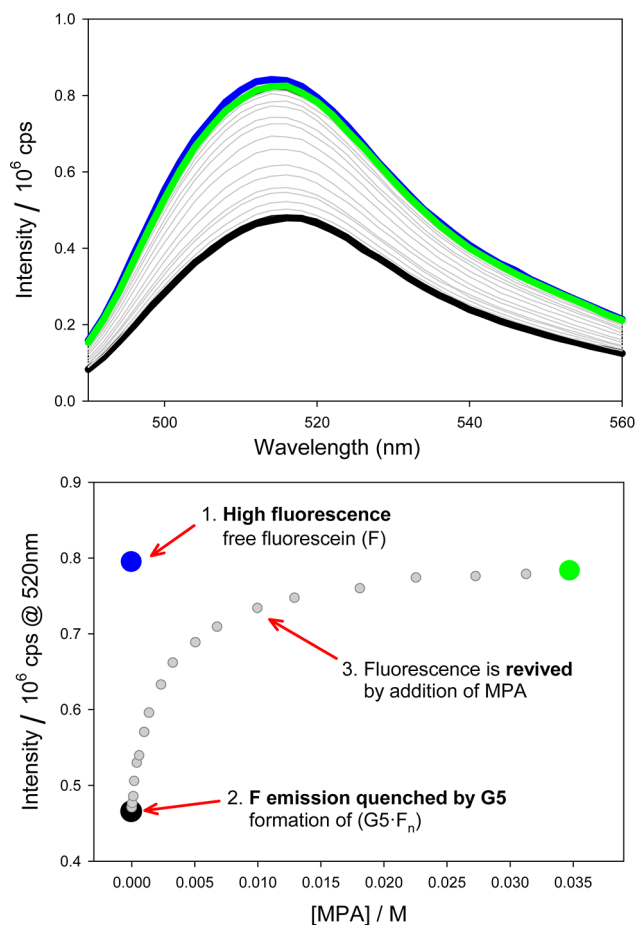


**Figure 4.** Fluorescence recovery upon binding of organophosphates. (Top) Emission spectra of solutions containing free fluorescein (blue), the (G5•F<sub>n</sub>) complex (black), and the complex in the presence of varying amounts of MPA (gray spectra, from black to green). (Bottom) Profile of the change in emission as a function of [MPA] at 520 nm ( $\lambda_{\text{ex}} = 485$  nm).

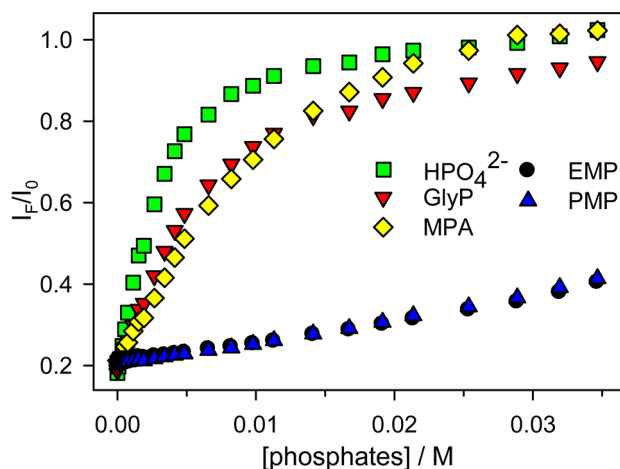


**Figure 5.** Displacement of fluorescein (F) from its (G5•F<sub>n</sub>) complex by GlyP, MPA, EMP, PMP and phosphate as a function of anion concentration. [F] =  $2.0 \times 10^{-6}$  M, [G5] =  $1.0 \times 10^{-6}$  M.

statistical methods for data reduction and classification, namely principal component analysis (PCA) and linear discriminant analysis (LDA).<sup>25</sup> Both algorithms are well established and

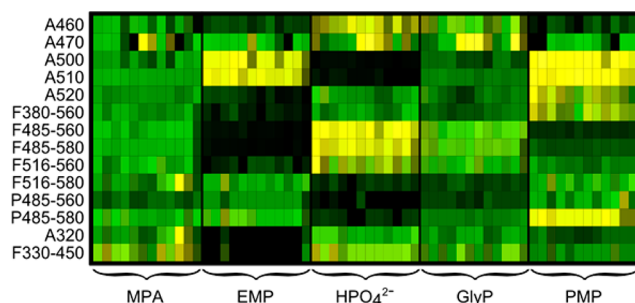


**Figure 6.** A visual map of the array's experimental response to the target phosphates ( $800 \mu\text{M}$ ), highlighting its rich cross-reactive behavior. "A" refers to an absorbance measurement, "F" to fluorescence emission, and "P" to fluorescence anisotropy.

implemented in common data analysis software (e.g., *Minitab*, *SyStat*, *Mathematica*, *Matlab*, *Origin PRO*, *SPSS*).

The experimental data set was then subjected to principal component analysis and data reduction. The resulting two-dimensional PCA score plot (Figure 7) shows clear clustering

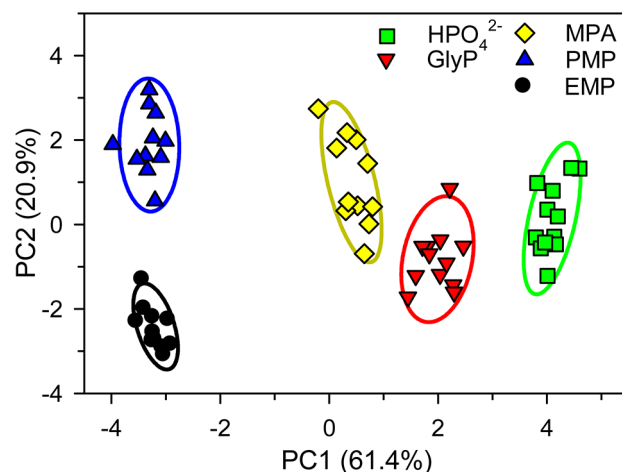


**Figure 7.** PCA score plot for the analysis of five phosphates at [analytes] =  $800 \mu\text{M}$ . Ellipsoids are drawn at 95% confidence.

of the data using only the first two principal components (representing 82.3% of the total variance), with excellent discriminatory capacity. The large distance between clusters in the PCA score plot reflects a significant differential response of the sensing system to the organophosphates.

In an attempt to take advantage of the information not captured by the first two principal components, we explored the use of three principal components instead. In this case the data can be represented in a three-dimensional plot (not shown), which would capture 90.6% of the total variance. Unfortunately, however, we observed no significant improvement in the clustering or dispersion; on the other hand, the 3D plot suffered from a marked reduction in readability, so we abandoned that route. Analyte concentrations higher than  $800 \mu\text{M}$  were also successfully subjected to analysis with results comparable to the  $800 \mu\text{M}$  case.

The PCA score plot in Figure 7 hints toward the chemical origin of the array's differential response. Two "superclusters" emerge at first glance, the first containing the PMP and EMP monoanions, and the second containing the MPA, GlyP and hydrogen phosphate dianions. Since the dendrimer is known to engage primarily in electrostatic interactions with its guests,<sup>22a</sup>

it makes good chemical sense that the major point of differentiation between these groups of anions is their charge. As the differentiation among these superclusters is most pronounced along PC1, we hypothesize that overall guest charge is a significant contributor to this component. It is also interesting to note that ethyl- (EMP) and pinacolyl methylphosphonate (PMP) are well differentiated by the array, even though their structures only differ in the phosphoester moiety. By the same token, it is also remarkable that methylphosphonate (MPA) and hydrogen phosphate are very clearly differentiated by the array as well.

Given the excellent clustering and classification shown above for an 800  $\mu\text{M}$  analyte concentration, we also tested the array's response to these analytes at a lower concentration (500  $\mu\text{M}$ ) (Figure 8). In this case, the first two principal components from

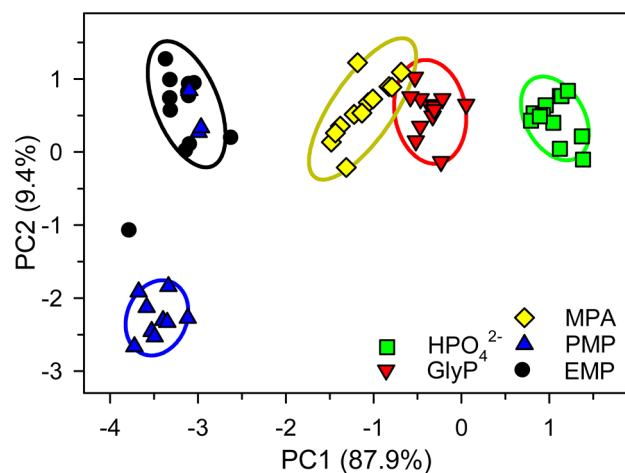


**Figure 8.** PCA score plot for the analysis of five phosphates at [analytes] = 500  $\mu\text{M}$ . Ellipsoids are drawn at 95% confidence.

PCA analysis captured 97.3% of the total variance. Although the classification accuracy inevitably decreased, the array was still able to discriminate between all analytes. Unsurprisingly, the system struggled to discriminate between the most similar among the analytes proposed, EMP and PMP, whose structural differences have little bearing on their interaction with the host.

The multidimensional response data set obtained at 800  $\mu\text{M}$  was further evaluated using linear discriminant analysis (LDA), a statistical method whose purpose is to provide the tightest clustering, separated by the largest possible intercluster distance. Indeed, a score plot constructed using the first two canonical factors obtained from LDA analysis shows excellent clustering and improved dispersion over the PCA results for the same data set (Figure 9). Furthermore, cross-validation routines can be used on LDA results to assess a system's ability to classify sample observations. In this case, a leave-one-out validation routine reported 100% accuracy for the classification of all organophosphates at 800  $\mu\text{M}$  concentration (see Supporting Information), an impressive results for such a simple system.

Once we verified that the minimal sensor array under investigation can differentiate the targeted organophosphates, we decided to use this method to measure analyte concentrations using this method. On the basis of the superior results obtained with LDA over PCA, we selected the former method for our quantitative studies, to make the most of the

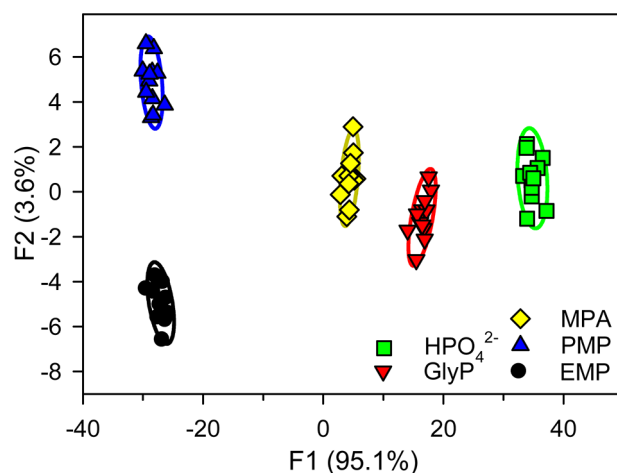


**Figure 9.** LDA score plot for the analysis of five phosphates at [analyte] = 800  $\mu\text{M}$ . Note the tighter clustering and improved dispersion over the PCA results on the same data set. Ellipsoids are drawn at 95% confidence.

small differences induced in the experimental data by changes in analyte concentration.

We first carried out a quantitative analysis of methylphosphonate (MPA) at concentrations ranging from 10  $\mu\text{M}$  to 2 mM. Six concentration values were selected in that range and eight replicates were measured for each concentration, for a total of 48 samples containing MPA. Linear discriminant analysis (LDA) was then applied to the concentration-dependent response. The resulting two-dimensional LDA score plot (Figure 10) yielded a clear separation of the clusters of

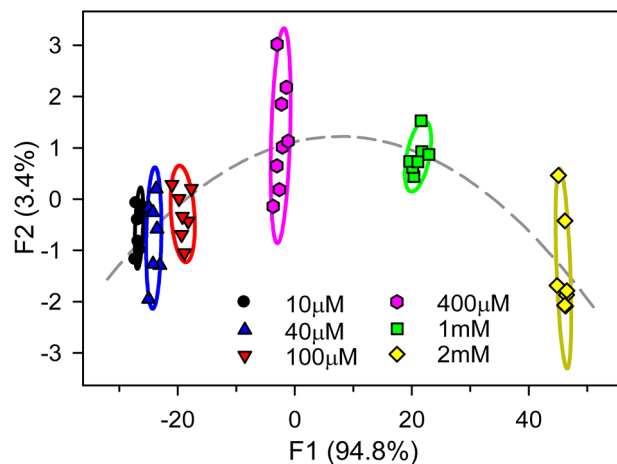


**Figure 10.** LDA score plot for the quantitative response of the sensor array to samples of methylphosphonate. [MPA] = 10  $\mu\text{M}$  to 2 mM. Ellipsoids are drawn at 95% confidence.

replicates, sorting them according to their concentration, and successfully accomplishing concentration-dependent discrimination. The process was repeated with comparable results for glyphosate (Figure 11) and  $\text{Na}_2\text{HPO}_4$  (see Supporting Information), attesting to the array's ability to determine the concentration of organic and inorganic phosphates of extensively different structures.

Jack-knife cross-validation routines showed 96% correct classification of individual samples according to their concentration for both methylphosphonate and glyphosate. In

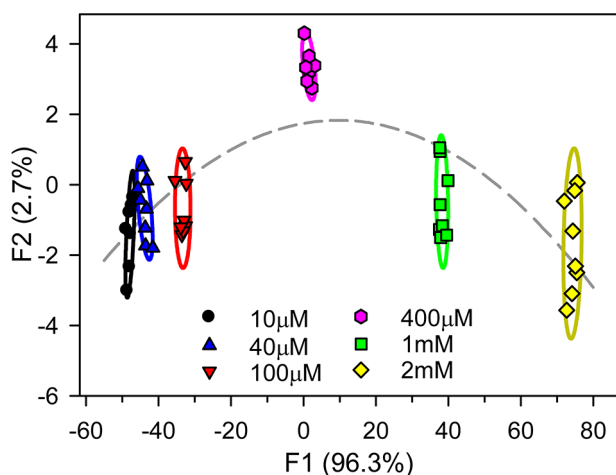


**Figure 11.** LDA score plot for the quantitative response of the sensor array to samples of glyphosate. [GlyP] = 10  $\mu\text{M}$  to 2 mM. Ellipsoids are drawn at 95% confidence.

both cases, one sample from each of the two lowest concentration clusters was misidentified (see Supporting Information for full validation results).

These positive outcomes encouraged us to attempt to use the system to identify an analyte and determine its concentration simultaneously. We concentrated on testing three representative organophosphates: methylphosphonate (MPA), the ultimate hydrolysis product of the sarin, soman and VX nerve gases; glyphosate (GlyP), a widely used organophosphate herbicide; and the inorganic hydrogen phosphate anion  $\text{HPO}_4^{2-}$ , a common nontoxic phosphate. These analytes were tested at nine concentrations, ranging from 10  $\mu\text{M}$  to 2 mM.

We analyzed the resulting data set with principal component and linear discriminant analysis to determine which algorithm best fit the problem at hand. Although LDA had given superior results in qualitative analyses (Figure 9), PCA turned out to be the better performer in this case. The PCA results were used to generate the concentration response functions shown in Figure 12. Each point on these curves was calculated by averaging the scores of all sample replicates from a specific analyte/

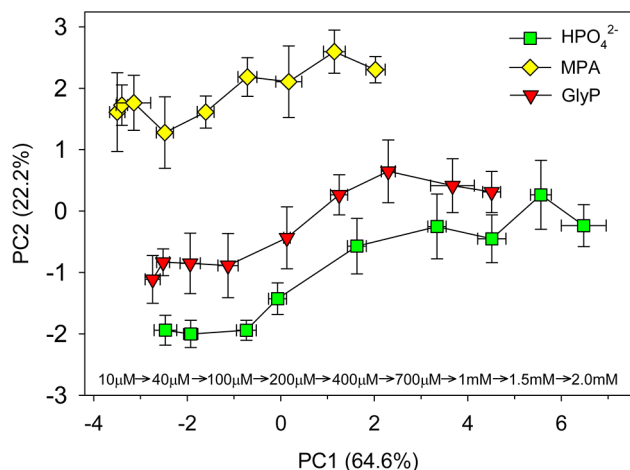


**Figure 12.** Response of the sensor array to three relevant phosphates over a concentration range spanning 10  $\mu\text{M}$  to 2 mM. Specific concentration values are indicated in the figure; concentration increases left-to-right in the plot.

concentration combination; the response functions were then represented as concentration-dependent “trajectories”.

It is worth noting at this point that, although these trajectories do describe the response of the array to a change in analyte concentration, they are not mere calibration curves; in fact, in addition to concentration information, these trajectories also contain information about the *identity* of each analyte. The trajectories shown in Figure 12 indicate that the nature of each analyte can be correctly identified even at concentrations at the lower end of the range. In short, the position of an unknown sample on the score plot provides information about both the nature and the concentration of the analyte that generated it. The data shown in Figure 12 demonstrates that the response from this two-component sensor array is both qualitative and quantitative: the array is able to discriminate three phosphates and report on their concentration over a wide range comprising 10  $\mu\text{M}$  to 2 mM.

As a point of reference, the U.S. Environmental Protection Agency has established a maximum contaminant level (MCL) of 0.7 mg/L for glyphosate in drinking water;<sup>26</sup> a 0.5 ppm guideline for sarin’s toxic threshold has long been established by the U.S. Department of the Army.<sup>27</sup> In this study, the limits of detection for GlyP, MPA, and  $\text{Na}_2\text{HPO}_4$  were found to be 0.5, 0.3, and 0.2 mg/L respectively, indicating that our method is sensitive enough to detect nerve gas simulants and hydrolysis products and herbicides at concentrations below levels that pose a health risk, so it can be used practically for simultaneous monitoring of multiple contaminants.

## CONCLUSIONS

We have demonstrated the use of a very simple sensor array including the two ( $\text{G5}\bullet\text{F}_n$ ) and ( $\text{G5}\bullet\text{MUP}_m$ ) sensing elements, prepared through self-assembly of commercially available starting materials, in itself a first for the detection of organophosphates. We showed that several organophosphates such as methylphosphonate, glyphosate, pinacolyl methylphosphonate, and ethyl methylphosphonate are successfully recognized by the array, and easily differentiated from inorganic phosphate: pattern recognition results (PCA, LDA) showed clean cluster resolution and excellent sample classification. Furthermore, we successfully performed quantitative analysis for a nerve agent simulant, a herbicide, and a ubiquitous phosphate, showing that our simple array was able to report on the nature and concentration of these compounds over a wide range (10  $\mu\text{M}$  to 2 mM).

To the best of our knowledge, this is the first case of recognition and quantitation of organophosphates in neutral aqueous solution using a sensing array assembled from commercially available building blocks. In view of the affordability and ready availability of the dendrimer and fluorescent indicators used here, and as a result of the modular nature of the self-assembled sensing ensembles used, we believe that these results pave the way for the development of simple high-throughput assays for the detection of organophosphates in environmental and safety applications.

## EXPERIMENTAL SECTION

Amine-terminated PAMAM dendrimers with ethylenediamine core of generation 5 were purchased from Dendritech, Inc. and received as MeOH solutions. 4-Methylumbelliferyl phosphate (MUP) and HEPES buffer (free acid) were purchased from VWR. Fluorescein, methylphosphonate, glyphosate, ethyl methylphosphonate, pinacolyl methylphosphonate and disodium phosphate were purchased from

Sigma-Aldrich. Materials were used as received without further purification. All experiments were carried out in water buffered to pH 7.4 with 4-(2-hydroxyethyl)-1-piperazineethanesulfonic acid (HEPES, 50 mM).

Displacement titrations such as that of the ( $G5 \bullet F_n$ ) ensemble with organophosphates reported in Figure 5 were carried out on benchtop instruments as well as on a microplate reader. In the former case, fluorescence measurements were carried out on an ISS PC1 spectrofluorimeter equipped with monochromators for wavelength selection and calibrated manual slits for resolution control, high-aperture Glan-Thompson calcite polarizers, and a 300 W high-pressure xenon arc lamp.

All the array spectroscopic data presented in this paper was acquired on a BioTek Synergy II multimode microwell plate reader, capable of measuring steady-state fluorescence intensity, fluorescence polarization (through bandpass filter sets and plastic sheet polarizers), and absorbance spectra (through a monochromator). Experiments were performed in nontreated (medium binding) 96-well plates with black walls and clear flat bottoms. Fluids were dispensed by hand using Eppendorf Research multichannel pipettors and disposable plastic tips.

In a typical pattern recognition experiment, the 96-well ( $12 \times 8$ ) plates were laid out as follows: one row was split between six free dye replicates and six  $G5$ -indicator replicates; a second row was filled with buffer to use as an optical blank. Five rows were used for the analytes of interest ( $Na_2HPO_4$ , GlyP, MPA, PMP and EMP).

The data acquired using the BioTek multimode microwell plate reader included single-wavelength absorbance, nonpolarized fluorescence emission, and fluorescence polarization measurements. In the case of fluorescence, the gain was adjusted automatically so that the highest reading from each plate reached 85% of the instrument full scale. Both absorbance and fluorescence emission raw data points were blanked by subtracting the average reading for the wells containing buffer. In the case of the ( $G5 \bullet F_n$ ) ensemble, absorbance was collected at the following wavelengths: 460, 470, 500, 510, and 520 nm. Fluorescence intensity was collected in the following channels ( $\lambda_{ex}/\lambda_{em}$ ): 380/560, 485/580, 485/560, 516/560, and 516/580 nm. Fluorescence anisotropy was collected in the following channels ( $\lambda_{ex}/\lambda_{em}$ ): 485/560, 485/580 nm. In the case of the ( $G5 \bullet MUP_m$ ) ensemble, absorbance was collected at 320 nm; fluorescence intensity was collected with excitation at 380 nm and emission at 450 nm. The data for qualitative and quantitative analyses were then processed without any further pretreatment, using the PCA and LDA algorithms implemented in the *Minitab* and *SyStat* software packages, respectively.

## ■ ASSOCIATED CONTENT

### ● Supporting Information

UV-visible and fluorescence spectra, binding and displacement studies on 4-methylumbelliferyl phosphates, further results from multivariate analysis and cross-validation methods, determination of limits of detection. This material is available free of charge via the Internet at <http://pubs.acs.org>.

## ■ AUTHOR INFORMATION

### Corresponding Author

marco.bonizzoni@ua.edu

### Notes

The authors declare no competing financial interest.

## ■ ACKNOWLEDGMENTS

We gratefully acknowledge the financial support of The University of Alabama faculty start-up funds.

## ■ REFERENCES

- (1) (a) Baylis, A. D. *Pest Manage. Sci.* **2000**, *56*, 299–308. (b) Duke, S. O.; Powles, S. B. *Pest Manage. Sci.* **2008**, *64*, 319–325.
- (2) Guy, M.; Singh, L.; Mineau, P. *Integr. Environ. Assess. Manage.* **2011**, *7*, 426–436.

- (3) Cedergreen, N.; Streibig, J. C. *Pest Manage. Sci.* **2005**, *61*, 1152–1160.

- (4) Thongprakaisang, S.; Thiantanawat, A.; Rangkadilok, N.; Suriyo, T.; Satayavivad, J. *Food Chem. Toxicol.* **2013**, *59*, 129–136.

- (5) (a) Chambers, J. E.; Oppenheimer, S. F. *Toxicol. Sci.* **2004**, *77*, 185–187. (b) Bajgar, J. In *Advances in Clinical Chemistry*; Academic Press: New York, **2004**; Vol. 38, pp 151–216.

- (6) Sambrook, M. R.; Notman, S. *Chem. Soc. Rev.* **2013**, *42*, 9251–9267.

- (7) (a) Black, R. M.; Read, R. W. *J. Chromatogr., A* **1998**, *794*, 233–244. (b) Pardasani, D.; Mazumder, A.; Gupta, A. K.; Kanaujia, P. K.; Tak, V.; Dubey, D. K. *Rapid Commun. Mass Spectrom.* **2007**, *21*, 3109–3114. (c) Read, R. W.; Black, R. M. *J. Chromatogr., A* **1999**, *862*, 169–177. (d) Richardson, D. D.; Caruso, J. A. *Anal. Bioanal. Chem.* **2007**, *388*, 809–823. (e) Smith, J. R.; Shih, M. L. *J. Appl. Toxicol.* **2001**, *21*, S27–S34.

- (8) (a) Xuan, W. M.; Cao, Y. T.; Zhou, J. H.; Wang, W. *Chem. Commun.* **2013**, *49*, 10474–10476. (b) Hartmann-Thompson, C.; Keeley, D. L.; Rousseau, J. R.; Dvornic, P. R. *J. Polym. Sci., Part A: Polym. Chem.* **2009**, *47*, 5101–5115. (c) Hewage, H. S.; Wallace, K. J.; Anslyn, E. V. *Chem. Commun.* **2007**, 3909–3911. (d) Wallace, K. J.; Fagbemi, R. I.; Folmer-Andersen, F. J.; Morey, J.; Lynth, V. M.; Anslyn, E. V. *Chem. Commun.* **2006**, 3886–3888. (e) Burnworth, M.; Rowan, S. J.; Weder, C. *Chem.—Eur. J.* **2007**, *13*, 7828–7836. (f) Dale, T. J.; Rebek, J. *J. Am. Chem. Soc.* **2006**, *128*, 4500–4501. (g) Knapton, D.; Burnworth, M.; Rowan, S. J.; Weder, C. *Angew. Chem., Int. Ed.* **2006**, *45*, 5825–5829. (h) Zhang, S. W.; Swager, T. M. *J. Am. Chem. Soc.* **2003**, *125*, 3420–3421. (i) Levitsky, I.; Krivoslykov, S. G.; Grate, J. W. *Anal. Chem.* **2001**, *73*, 3441–3448.

- (9) (a) Lee, J.; Seo, S.; Kim, J. *Adv. Funct. Mater.* **2012**, *22*, 1632–1638. (b) Walton, I.; Davis, M.; Munro, L.; Catalano, V. J.; Cragg, P. J.; Huggins, M. T.; Wallace, K. J. *Org. Lett.* **2012**, *14*, 2686–2689. (c) Wallace, K. J.; Morey, J.; Lynch, V. M.; Anslyn, E. V. *New J. Chem.* **2005**, *29*, 1469–1474.

- (10) (a) Horrillo, M. C.; Marti, J.; Matatagui, D.; Santos, A.; Sayago, I.; Gutierrez, J.; Martin-Fernandez, I.; Ivanov, P.; Gracia, I.; Cane, C. *Sens. Actuators, B* **2011**, *157*, 253–259. (b) Joshi, K. A.; Prouza, M.; Kum, M.; Wang, J.; Tang, J.; Haddon, R.; Chen, W.; Mulchandani, A. *Anal. Chem.* **2006**, *78*, 331–336. (c) Novak, J. P.; Snow, E. S.; Houser, E. J.; Park, D.; Stepnowski, J. L.; McGill, R. A. *Appl. Phys. Lett.* **2003**, *83*, 4026–4028. (d) Cattanaach, K.; Kulkarni, R. D.; Kozlov, M.; Manohar, S. K. *Nanotechnology* **2006**, *17*, 4123–4128.

- (11) (a) Arduini, F.; Neagu, D.; Dall'Oglio, S.; Moscone, D.; Palleschi, G. *Electroanalysis* **2012**, *24*, 581–590. (b) Shulga, O. V.; Palmer, C. *Anal. Bioanal. Chem.* **2006**, *385*, 1116–1123. (c) Tan, H. Y.; Loke, W. K.; Nguyen, N. T.; Tan, S. N.; Tay, N. B.; Wang, W.; Ng, S. H. *Biomed. Microdevices* **2014**, *16*, 269–275.

- (12) (a) Raj, V. B.; Singh, H.; Nimal, A. T.; Sharma, M. U.; Gupta, V. *Sens. Actuators, B* **2013**, *178*, 636–647. (b) Nieuwenhuizen, M. S.; Hartevelde, J. L. N. *Sens. Actuators, B* **1997**, *40*, 167–173.

- (13) Yang, Y. M.; Ji, H. F.; Thundat, T. *J. Am. Chem. Soc.* **2003**, *125*, 1124–1125.

- (14) Wang, D. Q.; Zhao, Q. T.; de Zoysa, R. S. S.; Guan, X. Y. *Sens. Actuators, B* **2009**, *139*, 440–446.

- (15) (a) Anzenbacher, P., Jr.; Palacios, M. A. In *Chemosensors: Principles, Strategies, and Applications*; Wang, B., Anslyn, E. V., Eds.; John Wiley & Sons, Inc.: Hoboken, NJ, **2011**; p 345–368. (b) Diehl, K. L.; Anslyn, E. V. *Chem. Soc. Rev.* **2013**, *42*, 8596–8611.

- (16) Minami, T.; Liu, Y.; Akdeniz, A.; Koutnik, P.; Esipenko, N. A.; Nishiyabu, R.; Kubo, Y.; Anzenbacher, P. *J. Am. Chem. Soc.* **2014**, *136* (32), 11396–11401.

- (17) (a) Pascual, L.; Campos, I.; Bataller, R.; Olguin, C.; Garcia-Breijo, E.; Martinez-Manez, R.; Soto, J. *Sens. Actuators, B* **2014**, *192*, 134–142. (b) Esipenko, N. A.; Koutnik, P.; Minami, T.; Mosca, L.; Lynch, V. M.; Zyryanov, G. V.; Anzenbacher, P. *Chem. Sci.* **2013**, *4*, 3617–3623. (c) Diaz de Grenu, B.; Moreno, D.; Torroba, T.; Berg, A.; Gunnars, J.; Nilsson, T.; Nyman, R.; Persson, M.; Pettersson, J.; Eklind, I.; Wasterby, P. *J. Am. Chem. Soc.* **2014**, *136*, 4125–4128. (d) Di Pietrantonio, F.; Benetti, M.; Cannata, D.; Verona, E.; Palla-

- Papavlu, A.; Dinca, V.; Dinescu, M.; Mattle, T.; Lippert, T. *Sens. Actuators, B* **2012**, *174*, 158–167. (e) Feng, L.; Musto, C. J.; Kemling, J. W.; Lim, S. H.; Suslick, K. S. *Chem. Commun.* **2010**, *46*, 2037–2039. (f) Lin, H. W.; Suslick, K. S. *J. Am. Chem. Soc.* **2010**, *132*, 15519–15521. (g) Ngo, K. A.; Lauque, P.; Aguir, K. *Sens. Mater.* **2006**, *18*, 251–260.
- (18) Mallet, A. M.; Liu, Y.; Bonizzoni, M. *Chem. Commun.* **2014**, *50*, 5003–5006.
- (19) Kataoka, M.; Tsuge, K.; Takesako, H.; Hamazaki, T.; Seto, Y. *Environ. Sci. Technol.* **2001**, *35*, 1823–1829.
- (20) (a) Kim, K.; Tsay, O. G.; Atwood, D. A.; Churchill, D. G. *Chem. Rev.* **2011**, *111*, 5345–5403. (b) Bartelt-Hunt, S. L.; Knappe, D. R. U.; Barlaz, M. A. *Crit. Rev. Environ. Sci. Technol.* **2008**, *38*, 112–136.
- (21) Nguyen, B. T.; Anslyn, E. V. *Coord. Chem. Rev.* **2006**, *250*, 3118–3127.
- (22) (a) Jolly, A. M.; Bonizzoni, M. *Supramol. Chem.* **2014**, DOI: 10.1080/10610278.2014.915971. (b) Bonizzoni, M.; Long, S. R.; Rainwater, C.; Anslyn, E. V. *J. Org. Chem.* **2012**, *77*, 1258–1266.
- (23) Szulc, A.; Appelhans, D.; Voit, B.; Bryszewska, M.; Klajnert, B. *New J. Chem.* **2012**, *36*, 1610–1615.
- (24) (a) Pritsch, K.; Raidl, S.; Marksteiner, E.; Blaschke, H.; Agerer, R.; Schloter, M.; Hartmann, A. *J. Microbiol. Methods* **2004**, *58*, 233–241. (b) Weiland, J. J.; Anderson, J. V.; Bigger, B. B. *Anal. Biochem.* **2007**, *361*, 140–142.
- (25) (a) Brereton, R. G. *Chemometrics for Pattern Recognition*; Wiley: Hoboken, NJ, 2009. (b) Szabo, A.; Boucher, K.; Jones, D.; Tsodikov, A. D.; Klebanov, L. B.; Yakovlev, A. Y. *Biostatistics* **2003**, *4*, 555–567. (c) Fukunaga, K. *Introduction to Statistical Pattern Recognition*; Academic Press: Boston, MA, 1990.
- (26) Technical Factsheet on: Glyphosate. <http://www.epa.gov/safewater/pdfs/factsheets/soc/tech/glyphosate.pdf> (accessed July 27, 2014).
- (27) United States Department of the Army In *Treatment of Chemical Warfare Casualties*; U.S. Government Print Office: Washington, DC, 1956; p 128.